Evaluation of the surface properties of 4-(Decyloxy) benzoic acid liquid crystal and its use in structural isomer separation

Birol IŞIK [ID], Fatih ÇAKAR [ID], Hüsnü CANKURTARAN [ID], Özlem CANKURTARAN* [ID]

Department of Chemistry, Faculty of Arts and Science, Yıldız Technical University, İstanbul, Turkey

Abstract: The selectivity of 4-(Decyloxy) benzoic acid (DBA) liquid crystal in surface adsorption region (303.2–328.2 K) and thermodynamic region (423.2 – 433.2 K) was investigated by inverse gas chromatography at infinite dilution (IGC-ID). The selectivity parameters of the structural isomer series named butyl acetate, butyl alcohol, and amyl alcohol series were calculated for the DBA using IGC-ID technique. Additionally, the surface properties including dispersive surface energy (γ_S^D), free energy (ΔG_A^S), enthalpy (ΔH_A^S), and acidity-basicity constants were calculated with net retention volumes obtained from IGC-ID experiment results. When the ΔH_A^S and ΔG_A^S are constants, DBA surface was found to be an acidic character ($K_D/K_A \cong 0.89$).

Key words: Inverse gas chromatography, liquid crystal, selectivity, surface properties

1. Introduction

The liquid crystal (LC) state, which is different from the known forms, was discovered in the 1888s during the studies of Reinitzer [1] and Lehmann [2] on some cholesterol esters. LC state, also called as the meso-phase, is known as a physical state located between the crystalline solid and the isotropic liquid phase. Although it is considered as a separate phase between the solid and liquid phase, it can have at least one property of the solid and liquid phase. In the LC structure, the spontaneous orientation of the molecules in a certain direction provides a geometric selectivity to the stationary phase [3–6]. The orientation of the molecules in the LC structure can also differentiate the properties and usage fields of the LC. LCs are widely used in sensor technology, technological devices, such as televisions, computers, tablets, and biological fields [7–10].

In the conventional gas chromatography (GC), certain stationary phases suitable for the chromatographic column studied are used. The probes in volatile form to be analysed in the GC are separated from each other depending on their polarity on conventional stationary phases. It is not possible to analyse high molecular weight and nonvolatile materials, such as LCs, polymers, composites, etc. in conventional GC [11–15]. Therefore, IGC-ID is a simple, low cost, high efficiency, and high accuracy technique developed to analyse such substances. This technique is based on filling the substances to be analysed into the chromatographic column as a stationary phase and retaining the probes passed over them in vapor form at different times [16–18].

Separation of the isomer series is crucial industrially. When LCs are used as stationary phase for separation of isomer series, generally better, more efficient results can be obtained compared to conventional stationary phases. By using the IGC-ID technique, faster and more accurate results can be obtained compared to conventional separation methods [19–23].

Surface properties are closely related to important physicochemical phenomena such as colloidal stability, stickiness, and wettability. Besides, the surface properties, especially the surface energy, is an extremely important parameters in understanding the interaction between the surface of the material and various probes [24–26]. Surface energy arises from unbalanced molecular forces on the surface of the materials. The surface energy of the materials can be analysed using liquid adsorption, flow microcalorimetry, and contact angle measurements. Since the application of these techniques is difficult and limited, IGC-ID has become a preferred technique by researchers [27–31].

In the scope of this study, DBA's ability to separate isomer series including butyl acetate series (n-butyl acetate (nBAc), iso-butyl acetate (iBAc) and tert-butyl acetate (tBAc)), butyl alcohol series (n-butyl alcohol (nBAl), iso-butyl alcohol (iBAl)

---

* Correspondence: kurtaran90@yahoo.com

and tert-butyl alcohol (tBAl)) and amyl alcohol series (n-amyl alcohol (nAAl), iso-amyl alcohol (iAAl) and tert-amyl alcohol (tAAl)), and surface properties were investigated by IGC-ID technique. The selectivity of DBA was investigated in surface adsorption (303.2–328.2 K) and thermodynamic region (423.2–433.2 K). Additionally, the IGC-ID experiments were carried out to investigate the surface properties of DBA in relation to polar and nonpolar probes in surface adsorption region (303.2–328.2 K). Using the retention data obtained from IGC-ID experiments, the parameters used to determine the selectivity parameters and the surface properties were calculated.

2. Theory of inverse gas chromatography at infinite dilution (IGC-ID)

2.1. The selectivity coefficient

To determine selectivity of materials, the net retention volumes (V_N) in surface adsorption region and thermodynamic region should be calculated as main data. For volatile polar and nonpolar solvents used in the analysis, the V_N is closely related to the interaction of these solvents with the materials [32–36]. V_N is calculated as follows:

$$V_N = Q.J.(t_R - t_A).T/T_f \tag{1}$$

Here, t_R and t_A are retention times of volatile probes and air, respectively; Q is the volumetric flow rate; T and T_f are the column and ambient temperature, respectively; J is James-Martin pressure correction factor.

The selectivity of the stationary phase contained in the chromatographic column can be calculated from the proportioning of the numerical difference between the retention times obtained from the IGC-ID experiments. Besides, selectivity coefficient can also be calculated from the ratio of V_N calculated according to Eq. (1). The selectivity of stationary phase is determined depending on the size of the selectivity coefficient (α). This value is calculated as follows [37,38]:

$$\alpha = (t_{R1} - t_A) / (t_{R2} - t_A) = V_{N1} / V_{N2} \tag{2}$$

Here, t_{R1} and t_{R2} are the retention time of the first and second isomer from the isomer pairs, respectively; t_A is the retention time of air; V_{N1} and V_{N2} are the net retention volume of the first and second isomer, respectively.

2.2. Surface properties

In recent years, IGC-ID is commonly used for examining the surface properties of the materials. The standard free energy (ΔG_A^o) value for the adsorption of volatile probes on the stationary phase is calculated with the help of the V_N resulting from the interaction between probe and stationary phase [39–41]. ΔG_A^o is calculated as follows:

$$\Delta G_A^o = - RT \, ln \, (V_N) + K \tag{3}$$

Surface energy is an extremely important parameter in explaining the interaction between stationary phase and volatile probes. The greater the surface energy, the more interactions between molecules. On the contrary, when this energy is low, the interaction decreases. Surface energy of the stationary phase (γ_S) can be calculated as a sum of dispersive energy (γ_S^D) generated by weak interactions on surface and specific energy (γ_S^S) generated by strong interactions on surface [42–44]:

$$\gamma_S = \gamma_S^S + \gamma_S^D \tag{4}$$

γ_S^D of stationary phase is determined when non-polar probes are injected at Henry's law region. This energy is due to dispersive interactions between molecules on the surface of the material and non-polar probe molecules [45]. γ_S^D values can be calculated in the surface adsorption region according to the method proposed by Dorris–Gray [46] as follows:

$$\gamma_S^D = (\Delta G_{[CH2]})^2 / 4(N_A)^2(a_{[CH2]})^2\gamma_{[CH2]} \tag{5}$$

Here, γ_S^D is the dispersive energy of the surface (mj/m²), $\Delta G_{[CH2]}$ is the adsorption free energy of a methylene group, which is determined the slope of the plot between the number of alkanes versus $RTlnV_N$ values, N_A is the Avogadro's number, $a_{[CH2]}$ is the molecular area of a methylene group (0.06 nm²) and $\gamma_{[CH2]}$ is the surface energy of a methylene group. $\gamma_{[CH2]}$ values are calculated at any temperature (t °C) as follows [47]:

$$\gamma_{[CH2]} = 35.6 - 0.058t \tag{6}$$

Additionally, the method proposed by Schultz is widely used to calculate dispersive energy of surface [48]. This energy is calculated as follows:

$$- RT \, ln \, (V_N) = 2N_A a(\gamma_S^D)^{0.5}(\gamma_L^D)^{0.5} + K \tag{7}$$

Here, a is the cross-sectional area of the probes, N_A is the Avogadro's number, γ_L^D is the dispersive energy of the probes. The a and γ_L^D values were taken from the literature, and were listed in Table 1. γ_S^D values of stationary phase can be calculated from the slope of plot between $RTlnV_N$ versus $a(\gamma_L^D)^{0.5}$ of non-polar probes.

$\Delta G_{[CH2]}$ values are calculated as follows [49]:

$$\Delta G_{[CH2]} = - RT \, ln \, (V_{N,n} /V_{N,n+1}) \tag{8}$$

Here, R is the universal gas constant; $V_{N,n}$ and $V_{N,n+1}$ are the net retention volumes of two n-alkanes having n and $n+1$ carbon atoms, respectively.

ΔG_A^S for the polar probes are calculated as follows:

$$\Delta G_A^S = - RT \, ln \, (V_N /V_{N(ref)}) \tag{9}$$

Table 1. The values of a and γ_L^D for non-polar and polar probes.

Probes	a($\times 10^{-10}$ m^2)	γ_L^D (mj/m^2)
n-Hexane (Hx)	51.5	18.4
n-Heptane (Hp)	57.0	20.3
n-Octane (O)	62.8	21.3
n-Nonane (N)	69.0	22.7
n-Decan (D)	75.0	23.4
Dichloromethane (DCM)	31.5	27.6
Chloroform (TCM)	44.0	25.9
Tetrahydrofuran (THF)	45.0	22.5
Ethyl acetate (EA)	48.0	19.6
Acetone (Ace)	42.5	16.5

When the studies are carried out at different temperatures, ΔH_A^S and ΔS_A^S values can be calculated as follows [50]:

$$\Delta G_A^S = \Delta H_A^S - T\Delta S_A^S \tag{10}$$

The value of ΔH_A^S is linked with K_A (donor or acidity group) and K_D (acceptor or basicity group) parameters. This situation is due to the interactions that occur between probes and surfaces that do not have dispersive and entropic interactions. These values are calculated as follows [51,52]:

$$-\Delta H_A^S = K_A(DN) + K_D(AN^*) \tag{11}$$

Here, DN is an electron donor or acidity number and AN^* is an electron acceptor or basicity number determined by Gutmann [53]. By calculating the value of ΔH_A^S for polar probes, a linear plot is drawn between $-\Delta H_A^S/AN^*$ and DN/AN^*. The values of K_A and K_D of solid materials can be obtained from the slope and intercept of the line, respectively. If $K_D/K_A > 1$, the surface is considered to be a basic; whereas, if $K_D/K_A < 1$, the surface is considered to be an acidic.

3. Materials and methods

All the properties of the chemicals used in this study are given in Table 2.

All measurements in IGC-ID studies were carried out using an Agilent Technologies HP-6890N device combined with thermal conductivity detector (TCD) (Hewlett-Packard, Palo Alto, CA, USA). The stainless-steel column (1/8" o.d., 2.10 mm i.d. 10 m) was purchased from Alltech Associates, Inc. (Chicago, IL, USA). Chromosorb W (AW-DMCS-treated, 80/100 mesh) was used as the support material and obtained from Sigma Aldrich. The DBA liquid crystal was dissolved in the Chloroform, and Chromosorb W was added slowly. A homogeneous mixture was obtained by continuous stirring in heating controlling water bath, and the LC was coated on support. Silane-treated glass wool used to plug the ends of the column was obtained from Alltech Associates Inc (Deerfield, IL, USA). The ends of the column were loosely plugged with silanized glass wool. After the column was cut to a size of 1 m and cleaned thoroughly, approximately 1.21 g of the prepared column interior material was filled. The total loading of DBA liquid crystal on the support was determined as 10.38% by weighing. Helium (He), which kept at a constant flow rate of 3.6 mL/min, was used as the mobile phase during the experiments. Probes and air were injected into the column with 1 mL and 10 mL Hamilton syringes, respectively. For infinite dilution, the probe (0.1 mL) was taken into the syringe and flushed into the air. Then, the retention times for probe and air were determined. At least four consecutive injections were made for each probe and air at each set of measurements.

4. Results and discussion

The main data (V_N) obtained from IGC-ID studies were calculated for all probes injected surface adsorption region (303.2–328.2 K) and thermodynamic region (423.2–433.2 K) according to Eq. (1). The retention diagrams of DBA used as separator stationary phase in two regions were given in Figure 1 and 2, respectively. The "α" values for nBAc/iBAc, nBAc/tBAc, nBAl/iBAl, nBAl/tBAl, nAAl/iAAl, and nAAl/tAAl were obtained using their V_N in two regions. "α" values calculated according to Eq. (2) determined the separation ability of DBA. The higher the values of the separation factor calculated according to Eq. (2), the better the selectivity for isomers. Table 3 and 4 shows the calculated the values for the isomer pairs in two regions. Considering these values, it is seen that isomers are separated. Besides, it was observed that structural isomers were better separated in the surface adsorption region than in the thermodynamic region.

Table 2. Source, assay, and CAS registry numbers of the chemicals.

Chemicals	Source	CAS No	Assay
DBA	Sigma Aldrich	5519-23-3	0.980
nBAc	Supelco	123-86-4	≥ 0.995
iBAc	Sigma Aldrich	110-19-0	≥ 0.980
tBAc	Sigma Aldrich	540-88-5	≥ 0.990
nBAl	Sigma Aldrich	71-36-3	≥ 0.994
iBAl	Supelco	78-83-1	≥ 0.990
tBAl	Sigma Aldrich	75-65-0	≥ 0.990
nAAl	Sigma Aldrich	71-41-0	≥ 0.990
iAAl	Sigma Aldrich	123-51-3	≥ 0.990
tAAl	Supelco	75-85-4	≥ 0.990
Hx	Supelco	110-54-3	≥ 0.997
Hp	Supelco	142-82-5	≥ 0.990
O	Sigma Aldrich	111-65-9	≥ 0.990
N	Sigma Aldrich	111-84-2	≥ 0.990
D	Sigma-Aldrich	124-18-5	≥ 0.940
EA	Supelco	141-78-6	≥ 0.998
Ace	Supelco	67-64-1	≥ 0.998
DCM	Supelco	75-09-2	≥ 0.998
THF	Supelco	109-99-9	≥ 0.998
TCM	Supelco	67-66-3	≥ 0.998

The main data (V_N) obtained from IGC-ID studies was calculated for all probes between 303.2 and 328.2 K according to Eq. (1). Retention diagrams of non-polar and polar probes were given in Figure 3 and 4, respectively.

The surface energy of a solid materials depends on the chemical structure, physical properties, and composition. Interactions between molecules on a solid surface and polar or nonpolar probe molecules are due to long- and short-range interactions known as weak interactions (London dispersive forces) and strong interactions (acid-base interactions). Dispersive surface energy occurs as a result of nonspecific interactions caused by the London dispersive forces known as weak or long-range interactions [54]. γ_S^D can be calculated using IGC-ID technique based on well-known approaches for data analysis, such as Dorris–Gray (Eq. (5)) and Schultz (Eq. (7)) methods. In these γ_S^D calculations, homologous alkane vapor series are used in infinite dilution, resulting in a single numerical γ_S^D value. ΔG_A for the all probes were calculated from the Schultz method using Eq. (7) in the surface adsorption region (303.2–328.2 K). A plot of $RTlnV_N$ versus $a(\gamma_L^D)^{0.5}$ for all probes was plotted at 303.2 K in Figure 5. From Eqs. (5) and (7), γ_S^D of DBA was calculated using Schultz and Dorris-Gray methods. The results obtained from studies were listed in Table 5.

It is showed that the value determined for γ_S^D of DBA have different ranges from 47.51–44.06 (Schultz method) to 47.74–46.19 mj/m^2 (Dorris-Gray method). Besides, it is observed that the γ_S^D values calculated by Dorris-Gray method are higher than those obtained from the Schultz method. The γ_S^D values obtained from the Schultz method decrease faster than the γ_S^D values obtained by the Dorris–Gray method with increasing temperature. The results obtained for the Schultz and Dorris–Gray method at surface adsorption region are close to each other, showing that these two methods are compatible and feasible. There is no study on DBA in the literature. A rough comparison can be made with reported LCs. In the literature, γ_S^D values for LCs were ranged from 30 to 42 mj/m^2 in agreement with this study [50, 55].

The values of $-\Delta G_A^S$ were calculated by the numerical difference between the calculated value of $RTlnV_N$ and that which was obtained from Eq. (7) of the linear plot of the nonpolar reference line. The variation of ΔG_A^S between DBA and the polar probes for the studied temperatures is given in Table 6. Regarding the Table 6, it was seen that the temperature did not change the ΔG_A^S values much. ΔH_A^S values were calculated for polar probes and the results were given in Table 7. The ΔH_A^S values were calculated as the degree of interaction between the DBA molecule surface and the polar probe
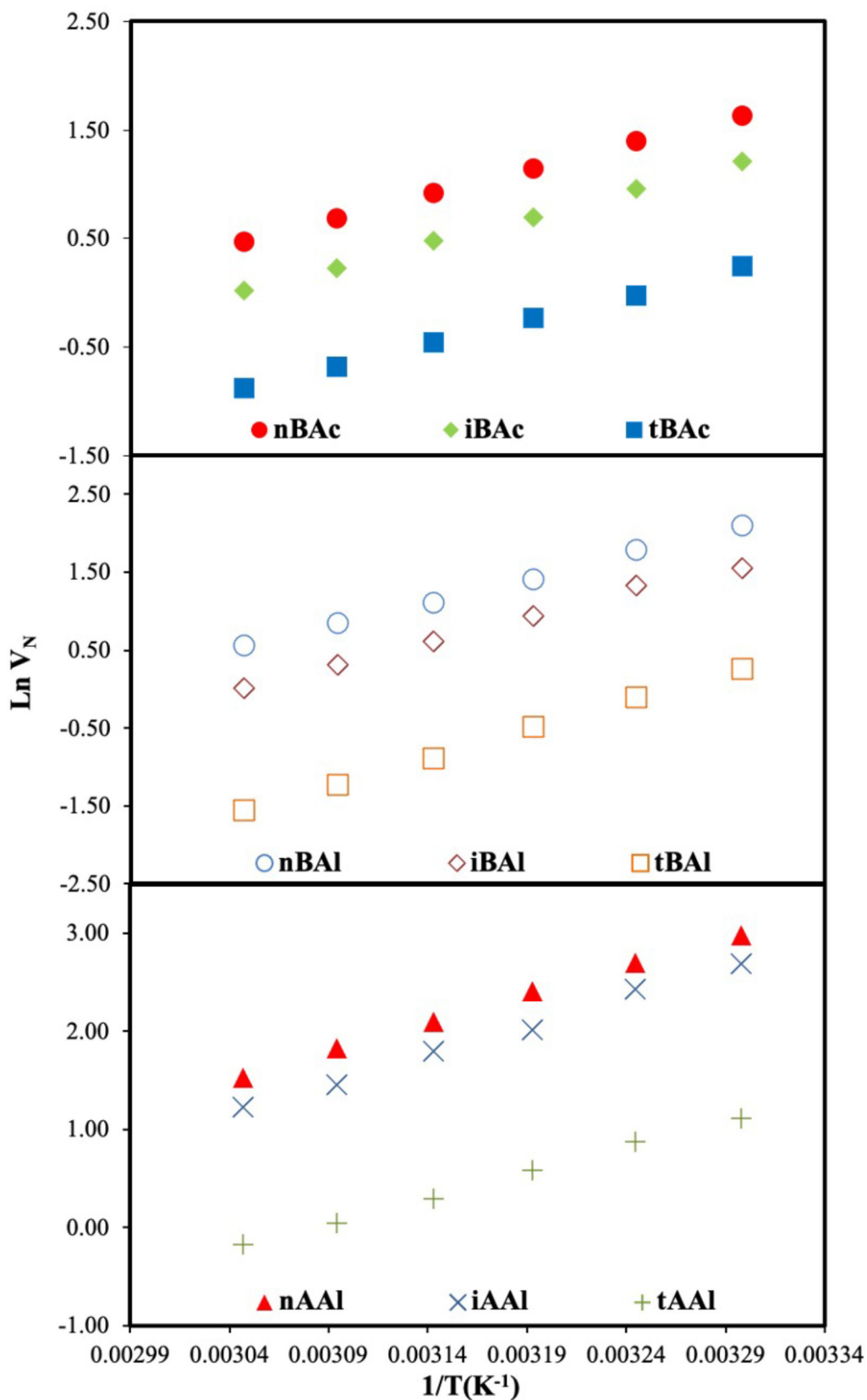
Figure 1. Net retention volumes (V_N) of isomer series on DBA (Surface adsorption region).
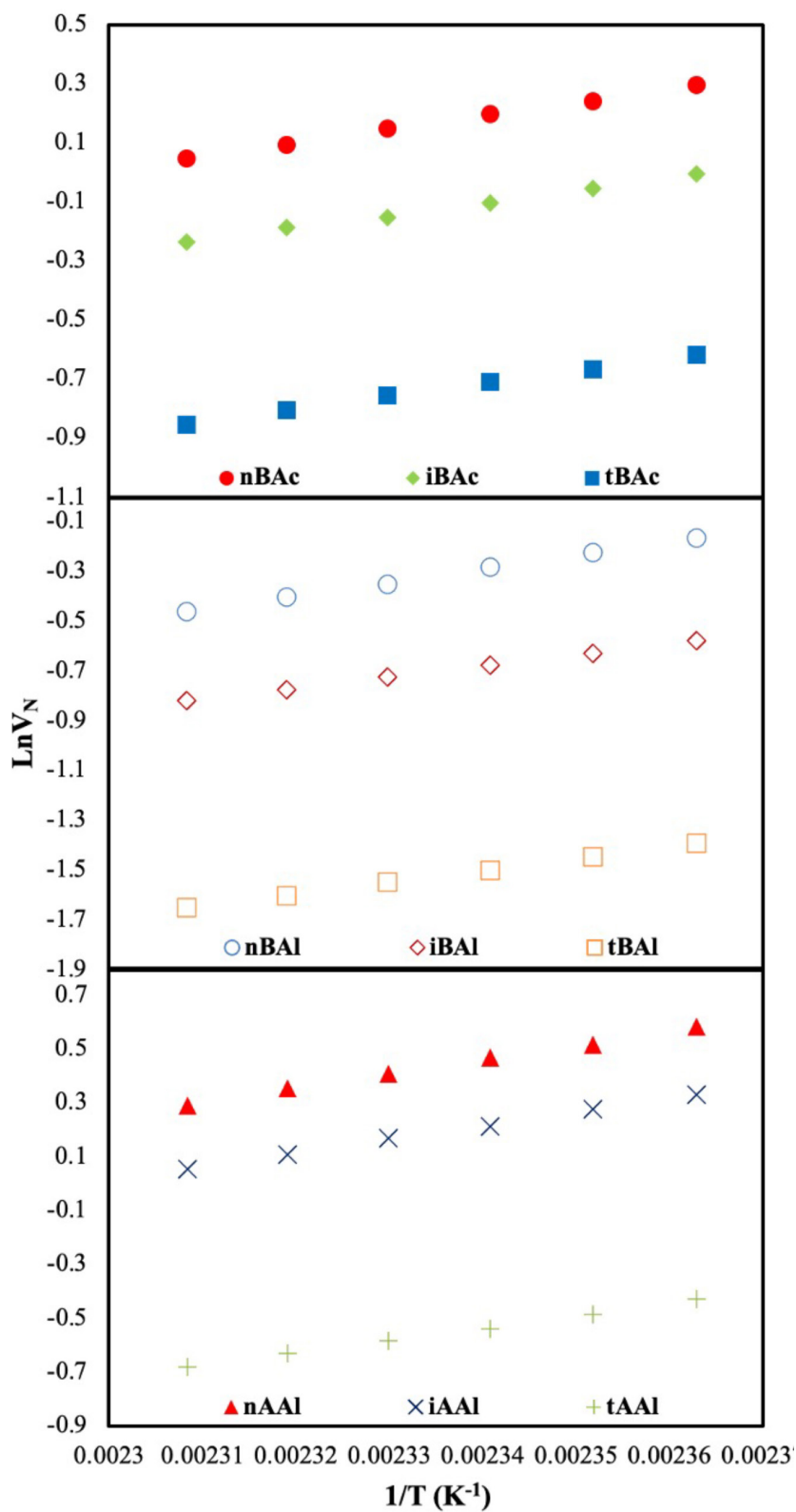
Figure 2. Net retention volumes (V_N) of isomer series on DBA (Thermodynamic region).

Table 3. The separation factor of DBA for the isomer pairs: nBAc/iBAc, nBAc/tBAc, nBAl/iBAl, nBAl/tBAl, nAAl/iAAl, and nAAl/tAAl (303.2–328.2 K).

$\alpha = V_{N1} / V_{N2}$						
T (K)	V_{NnBAc} / V_{NiBAc}	V_{NnBAc} / V_{NtBAc}	V_{NnBAl} / V_{NiBAl}	V_{NnBAl} / V_{NtBAl}	V_{NnAAl} / V_{NiAAl}	V_{NnAAl} / V_{NtAAl}
303.2	1.52	3.99	1.72	6.26	1.34	6.49
308.2	1.55	4.15	1.58	6.69	1.31	6.19
313.2	1.57	3.98	1.60	6.66	1.48	6.20
318.2	1.57	4.00	1.65	7.41	1.35	6.03
323.2	1.58	3.90	1.70	7.89	1.46	5.97
328.2	1.57	3.88	1.74	8.34	1.35	5.46

Table 4. The separation factor of DBA for the isomer pairs: nBAc/iBAc, nBAc/tBAc, nBAl/iBAl, nBAl/tBAl, nAAl/iAAl, and nAAl/tAAl (423.2–433.2 K).

$\alpha = V_{N1} / V_{N2}$						
T (K)	V_{NnBAc} / V_{NiBAc}	V_{NnBAc} / V_{NtBAc}	V_{NnBAl} / V_{NiBAl}	V_{NnBAl} / V_{NtBAl}	V_{NnAAl} / V_{NiAAl}	V_{NnAAl} / V_{NtAAl}
423.2	1.35	2.50	1.52	3.40	1.29	2.75
425.2	1.35	2.51	1.51	3.33	1.27	2.71
427.2	1.36	2.49	1.49	3.45	1.29	2.76
429.2	1.35	2.47	1.45	3.38	1.28	2.70
431.2	1.33	2.44	1.46	3.35	1.28	2.70
433.2	1.33	2.44	1.43	3.32	1.26	2.63
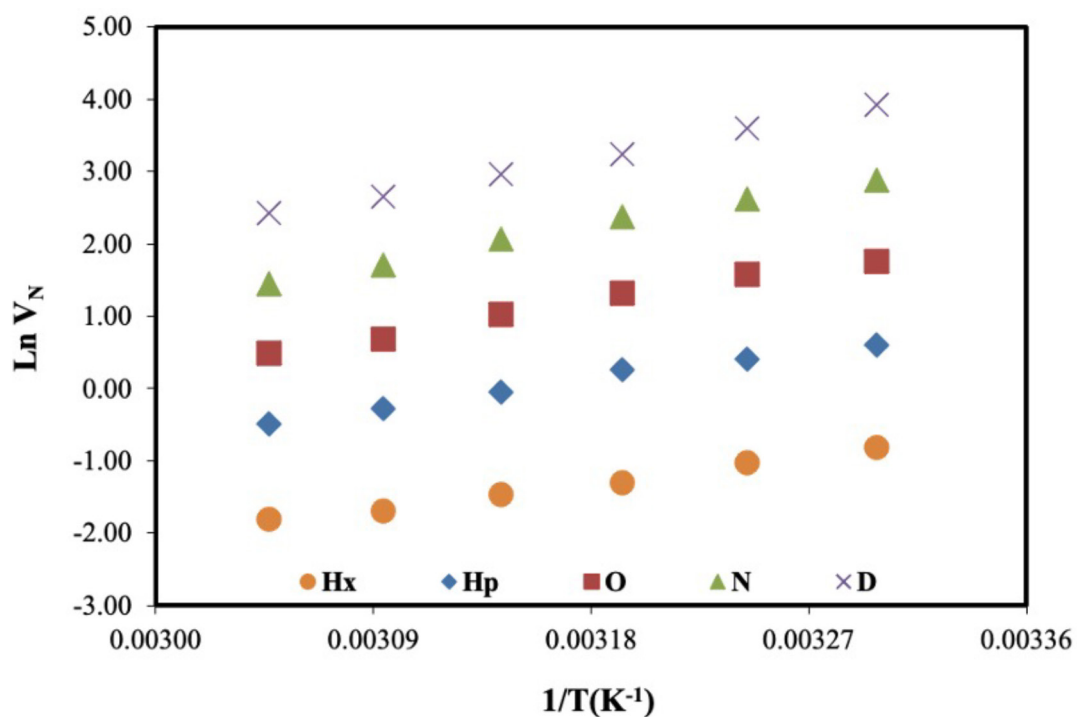
Figure 3. Net retention volumes (V_N) of nonpolar probes on DBA.
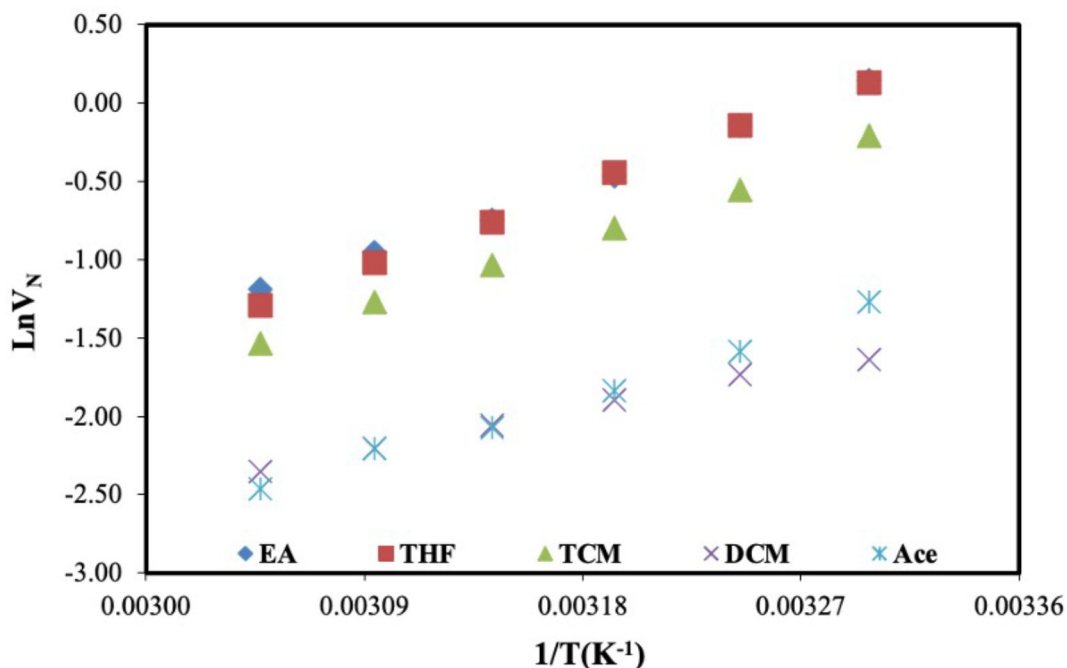
Figure 4. Net retention volumes (V_N) of polar probes on DBA.
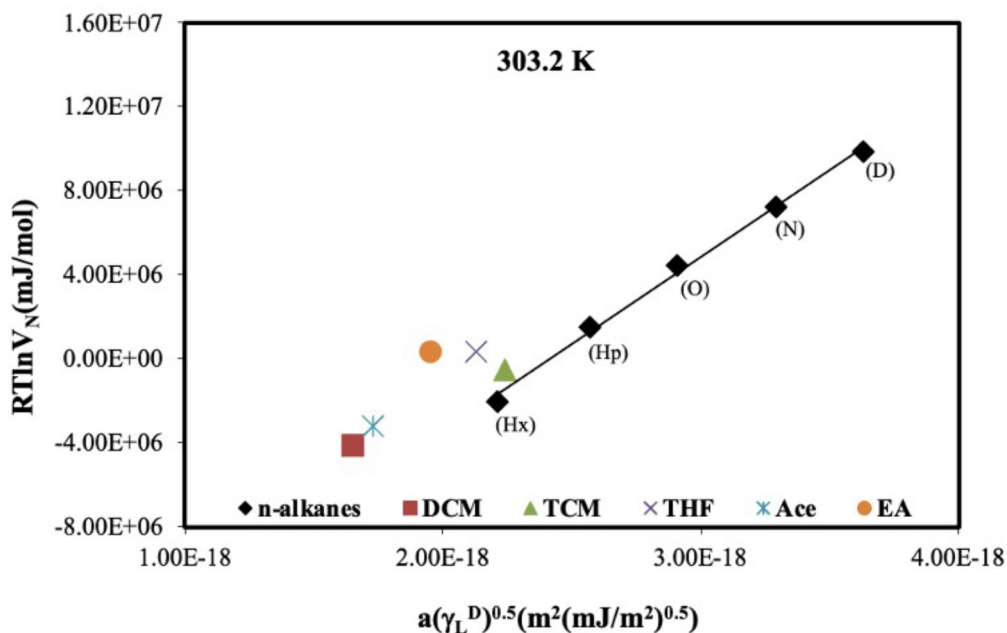
Figure 5. A linear plot of $RTlnV_N$ vs $a(\gamma_L^D)^{0.5}$ for all probes on DBA at 303.2 K.

molecules. These values were followed the order THF>EA>Ace>TCM>DCM. The DCM probe molecule ($DN = 0.0$, $AN = 16.4$) showed the lowest $-\Delta H_A^S$ value which is to be expected taking into account the acidic properties of this molecule and the acidic properties of LC surface given by the K_A value. THF is a basic probe molecule ($DN = 84.4$, $AN = 2.1$), it may be expected to interact strongly with acid surfaces [56,57]. Considering the values of ΔH_A^S and ΔG_A^S for each polar probe, adsorption occurs exothermically and spontaneously for all studied temperatures. The specific intermolecular interactions are derived from the interaction between the polar probe and the Lewis acidic-basic sites on surface [58–60].

Table 5. Dispersive surface energy (γ_S^D) of DBA.

T (K)	γ_S^D $mj.m^{-2}$	
	Schultz	Dorris-Gray
303.2	47.51	47.74
308.2	47.06	47.69
313.2	46.38	47.36
318.2	45.89	47.27
323.2	44.71	46.45
328.2	44.06	46.19

Table 6. The variation of free energy of specific interactions, $-\Delta G_A^S$ (kj/mol), between DBA and the polar probes for the studied temperatures.

T (K)	EA	Ace	DCM	TCM	THF
303.2	4.21	2.48	2.21	0.91	2.69
308.2	3.99	2.10	2.39	0.54	2.50
313.2	3.68	1.92	2.42	0.45	2.28
318.2	3.54	1.83	2.53	0.42	2.03
323.2	3.63	2.03	2.67	0.44	2.00
328.2	2.95	1.24	2.17	-0.34	1.21

Table 7. Values of enthalpy (ΔH_A^S) of adsorption on DBA for the polar probes.

Polar probes	$-\Delta H_A^S$ (kj/mol)
Ace	13.68
EA	17.20
THF	18.39
DCM	0.87
TCM	12.12

A plot of $-\Delta H_A^S/AN^*$ versus DN/AN^* was plotted by K_A as the slope and K_D as the intercept using Eq. (11), and it is shown in Figure 6. The character of DBA surface was determined by the ratio of K_D/K_A. The obtained K_A and K_D values were listed in Table 8. Due to the K_D/K_A value is lower than 1, DBA surface is an acidic character.

5. Conclusion

IGC-ID technique was used to investigate the separation of isomer series in surface adsorption (303.2–328.2 K) and thermodynamic region (423.2–433.2 K) and the surface properties of DBA in surface adsorption region. Considering the separation factors, it was determined that the DBA in IGC-ID technique can be used to separate the isomer series in surface adsorption and thermodynamic region. The values of γ_S^D for DBA were determined to be 47.51–44.06 mj/m^2 using the Schultz method and 47.74–46.19 mj/m^2 using the Dorris–Gray method. γ_S^D values from both calculation methods decrease linearly with the increase in temperature in the range from 303.2 to 328.2 K. The values of K_A and K_D were found to be 0.2134 and 0.1907, respectively. As shown that, the K_D value is lower than the K_A. In this case, it can be said that
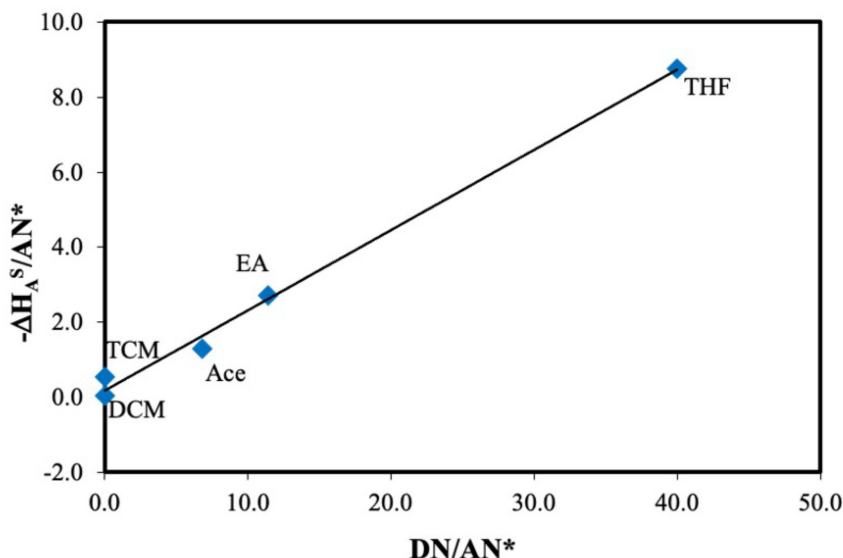
Figure 6. The plot of $-\Delta H_A^S/AN^*$ vs DN/AN^*.

Table 8. Lewis acid-base parameters, K_A and K_D, of DBA.

Liquid crystal	K_A	K_D	K_D/K_A
DBA	0.2134 ± 0.012	0.1907 ± 0.009	0.89

the DBA surface is an acidic character. The IGC-ID technique is very important in improving the quality of products for industrial fields, since isomers can be separated effectively and the surface energy of samples can be easily determined.

References

1. Reinitzer F. Beiträge zur Kenntniss des Cholesterins. Monatshefte für chemie und verwandte teile anderer wissenschaften 1888; 9: 421-441. doi: 10.1007/BF01516710 (in German).

2. Lehmann O. Uber fliessende krystalle. zeitschrift für physikalische chemie 1889; 4 (1): 462-472. doi: 10.1515/zpch-1889-0434 (in German).

3. Khodja FA, Sassiat P, Hanafi M, Thiebaut D, Vial J. A promising "metastable" liquid crystal stationary phase for gas chromatography. Journal of Chromatography A 2020; 1616: 460786. doi: 10.1016/j.chroma.2019.460786

4. Witkiewicz Z, Oszczudlowski J, Pepelewicz M. Liquid-crystalline stationary phase for gas chromatography. Journal of Chromatography A 2005; 1062 (2): 155-174. doi: 10.1016/j.chroma.2004.11.042

5. Akkurt N, Al-Jumaili MHA, Ocak H, Cakar F, Torun L. Synthesis and liquid crystalline properties of new triazine-based p-conjugated macromolecules with chiral side groups. Turkish Journal of Chemistry 2020; 44: 726-735. doi: 10.3906/kim-1912-51

6. Akkurt N, Al-Jumaili MHA, Bilgin Eran B, Ocak H, Torun L. Acetylene-bridged triazine p-conjugated structures: synthesis and liquid crystalline properties. Turkish Journal of Chemistry 2019; 43: 1436-1444. doi: 10.3906/kim-1907-26.

7. Çağlar FP, Akdaş-Kılıç H, Ocak H, Bilgin Eran B. Chiral polymorphism in new imine based rod-like liquid crystals. Journal of Molecular Structure 2020; 1220: 128755. doi: 10.1016/j.molstruc.2020.128755

8.   Kato T, Mizoshita N, Kishimoto K. Functional liquid-crystalline assemblies: self-organized soft materials. Angewandte Chemie International Edition 2006; 45 (1): 38-68. doi: 10.1002/anie.200501384

9.   Cakar F, Ocak H, Ozturk E, Mutlu-Yanic S, Kaya D, San N, Cankurtaran O, Bilgin-Eran B, Karaman F. Investigation of thermodynamic and surface characterization of 4-[4-(2-ethyl hexyloxy) benzoyloxy] benzoic acid thermotropic liquid crystal by inverse gas chromatography. Liquid Crystals 2014; 41 (9): 1323-1331. doi: 10.1080/02678292.2014.919672

10. Ocak H, Özerol EA, Çelikel FÇ, Okutan M, Bilgin Eran B. The synthesis, mesomorphic and dielectric investigation of new unsymmetrical bent-core mesogens derived from 3-hydroxybenzoic acid. Chemical Papers 2020; 74: 3899-3911. doi: 10.1007/s11696-020-01203-4

11. Adiguzel AC, Cakar F, Senkal BF, Cankurtaran O, Hepuzer Gursel Y, Karaman F. Determination of glass transition temperature and surface properties of novel chalcone modified poly (styrene) based polymer. Thermal Science 2019; 23 (1): 193-202. doi: 10.2298/TSCI180912343A

12. Cankurtaran O, Yilmaz F. A study of the thermodynamical interactions of bisphenol-A polycarbonate with some solvents by gas chromatography. Turkish Journal of Chemistry 1997; 21: 401-408.

13. Adamska K, Sandomierski M, Buchwald Z, Voelkel A. Inverse gas chromatography in the examination of surface properties of experimental dental composites. Polymer Testing 2020; 90: 106697. doi: 10.1016/j.polymertesting.2020.106697

14. Khodakarami M, Alagha L, Burnett DJ. Probing surface characteristics of rare earth minerals using contact angle measurements, atomic force microscopy, and inverse gas chromatography. ACS Omega 2019; 4 (8): 13319-13329. doi: 10.1021/acsomega.9b01491

15. Yazici O, Ocak H, Cakar F, Cankurtaran O, Bilgin-Eran B, Karaman F. Synthesis and thermodynamical interactions of (S)-5-(2-methylbutoxy)-2-[[[4-hexyloxyphenyl] imino] methyl]-phenol liquid crystal with some solvents. Optoelectronics and Advanced Materials-Rapid Communications 2008; 2 (6): 366-370.

16. Tamayo A, Pena-Alonso R, Rubio J, Raj R, Soraru GD, Oteo JL. Surface energy of sol gel-derived silicon oxycarbide glasses. The American Ceramic Society 2011; 94 (12): 4523-4533. doi: 10.1111/j.1551-2916.2011.04810.x

17. Grajek H, Witkiewicz Z, Purchala M, Drzewinski W. Liquid crystals as stationary phases in chromatography. Chromatographia 2016; 79: 1217-1245. doi: 10.1007/s10337-016-3154-5

18. Belusso AC, Strack ML, Guadagnin LS, Faccin DJL, Cardozo NSM, Soares RP, Staudt PB. Infinite dilution activity coefficient of solvents in poly-3-hydroxybutyrate from inverse gas chromatography. Fluid Phase Equilibria 2020; 522: 112742. doi: 10.1016/j.fluid.2020.112742

19. Witkiewicz Z, Szulc J, Dabrowski R. Disc-like liquid crystalline stationary phases from the triphenylene derivatives group. Journal of Chromatography A 1984; 315: 145-159. doi: 10.1016/S0021-9673(01)90732-0

20. Witkiewicz Z. Application of liquid crystals in chromatography. Journal of Chromatography A 1989; 466: 37-87. doi: 10.1016/S0021-9673(01)84616-1

21. Ghanem E, Al-Hariri S. Separation of isomers on nematic liquid crystal stationary phases in gas chromatography: a review. Chromatographia 2014; 77: 653-662. doi: 10.1007/S10337-014-2675-z

22. Cook LE, Spangelo RC. Separation of monosubstituted phenol isomers using liquid crystals. Analytical Chemistry 1974; 46 (1): 122-125. doi: 10.1021/ac60337a020

23. Richmond AB. Use of liquid crystals for the separation of position isomers of disubstituted benzenes. Journal of Chromatographic Science 1971; 9 (9): 571-574. doi: 10.1093/chromsci/9.9.571

24. Ban T, Li XP, Li CL, Wang Q. Surface characterization of a series of 1-alkyl-3-methylimidazolium based ionic liquids by inverse gas chromatography. Industrial & Engineering Chemistry Research 2018; 57 (36): 12249-12253. doi: 10.1021/acs.iecr.8b02110

25. Menzel R, Bismarck A, Shaffer MSP. Deconvolution of the structural and chemical surface properties of carbon nanotubes by inverse gas chromatography. Carbon 2012; 50 (10): 3416-3421. doi: 10.1016/j.carbon.2012.02.094

26. Cordeiro N, Gouveia C, John MJ. Investigation of surface properties of physico-chemically modified natural fibres using inverse gas chromatography. Industrial Crops and Products 2011; 33 (1): 108-115. doi: 10.1016/j.indcrop.2010.09.008

27. Krol P, Krol B. Determination of free surface energy values for ceramic materials and polyurethane surface-modifying aqueous emulsions. Journal of The European Ceramic Society 2006; 26 (12): 2241-2248. doi: 10.1016/j.jeurceramsoc.2005.04.011

28. Aşkın A, Topaloğlu Yazıcı D. Surface characterization of sepiolite by inverse gas chromatography. Chromatographia 2005; 61: 625-631. doi: 10.1365/s10337-005-0558-z

29. Sivaev IB, Bregadze VI. Lewis acidity of boron compounds. Coordination Chemistry Reviews 2014; 270-271: 75-88. doi: 10.1016/j.ccr.2013.10.017

30. Perez-Mendoza M, Almazan-Almazan MC, Mendez-Linan L, Domingo-Garcia M, Lopez-Garzon FJ. Evaluation of the dispersive component of the surface energy of active carbons as determined by inverse gas chromatography at zero surface coverage. Journal of Chromatography A 2008; 1214 (1-2): 121-127. doi: 10.1016/j.chroma.2008.10.070

31. Planinsek O, Trojak A, Srcic S. The dispersive component of the surface free energy of powders assessed using inverse gas chromatography and contact angle measurement. International Journal of Pharmaceutics 2001; 221 (1-2): 211-217. doi: 10.1016/S0378-5173(01)00687-1

32. Kunaver M, Zadnik J, Planinsek O, Srcic S. Inverse gas chromatography – a different approach to characterization of solids and liquids. Acta Chimica Slovenica 2004; 51: 373-394.

33. Voelkel A, Strzemiecka B, Marek AA, Zawadiak J. Inverse gas chromatography investigation of oxidized polyolefins: surface properties. Journal of Chromatography A 2014; 1337: 194-201. doi: 10.1016/j.chroma.2014.02.042

34. Ugraskan V, Isik B, Yazici O, Cakar F. Thermodynamic characterization of sodium alginate by inverse gas chromatography. Journal of Chemical & Engineering Data 2020; 65: 1795-1801. doi: 10.1021/acs.jced.9b01074

35. Cakar F. Synthesis and thermodynamic characterization of poly(methyl methacrylate)/multiwall carbon nanotube nanocomposite. Surface and Interface Analysis 2020; 1: 1-10. doi: 10.1002/sia.6911

36. Pal A, Kondor A, Mitra S, Thu K, Harish S, Saha BB. On surface energy and acid-base properties of highly porous parent and surface treated activated carbons using inverse gas chromatography. Journal of Industrial and Engineering Chemistry 2019; 69: 432-443. doi: 10.1016/j.jiec.2018.09.046

37. Ocak H, Mutlu-Yanic S, Cakar F, Bilgin-Eran B, Guzeller D, Karaman F, Cankurtaran O. A study of the thermodynamical interactions with solvents and surface characterization of liquid crystalline 5-((S)-3,7-dimethyloctyloxy)-2-[[[4-(dodecyloxy) phenyl] imino]-methyl] phenol by inverse gas chromatography. Journal of Molecular Liquids 2016; 223: 861-867. doi: 10.1016/j.molliq.2016.09.002

38. Katja DW, Werner E. Theory of gas chromatography. In: Dettmer-Wilde K, Engewald W (editors). Practical Gas Chromatography. Berlin: Springer-Verlag, 2014, pp. 21-31.

39. Carmona-Quiroga PM, Rubio J, Sanchez MJ, Martinez-Ramirez S, Blanco-Varela MT. Surface dispersive energy determined with IGC-ID in anti-graffiti-coated building materials. Progress in Organic Coatings 2011; 71: 207-212. doi: 10.1016/j.porgcoat.2011.02.014

40. Autie-Castro G, Reguera E, Cavalcante Jr. CL, Araujo AS, Rodriguez-Castellon E. Surface acid-base properties of Cu-BTC and Fe-BTC MOFs. An inverse gas chromatography and n-butylamine thermo desorption study. Inorganica Chimica Acta 2020; 507: 119590. doi: 10.1016/j.ica.2020.119590

41. Belgacem MN, Czeremuszkin G, Sapieha S, Gandini A. Surface characterization of cellulose fibres by XPS and inverse gas chromatography. Cellulose 1995; 2: 145-157. doi: 10.1007/BF00813015

42. Adamska K, Sandomierski M, Buchwald Z, Voelkel A. Inverse gas chromatography in the examination of surface properties of experimental dental composites. Polymer Testing 2020; 90: 106697. doi: 10.1016/j.polymertesting.2020.106697

43. Shah UV, Olusanmi D, Narang AS, Hussain MA, Tobyn MJ, Heng JYY. Decoupling the contribution of dispersive and acid-base components of surface energy on the cohesion of pharmaceutical powders. International Journal of Pharmaceutics 2014; 475: 592-596. doi: 10.1016/j.ijpharm.2014.09.018

44. Shah UV, Olusanmi D, Narang AS, Hussain MA, Gamble JF, Tobyn MJ, Heng JYY. Effect of crystal habits on the surface energy and cohesion of crystalline powders. International Journal of Pharmaceutics 2014; 472 (1-2): 140-147. doi: 10.1016/j.ijpharm.2014.06.014

45. Bensalem S, Hamdi B, Confetto SD, Calvet R. Characterization of surface properties of chitosan/bentonite composites beads by inverse gas chromatography. International Journal of Biological Macromolecules 2021; 166: 1448-1459. doi: 10.1016/j.ijbiomac.2020.11.024

46. Dorris GM, Gray DG. Adsorption of n-alkanes at zero surface coverage on cellulose paper and wood fibers. Journal of Colloid and Interface Science 1980; 77 (2): 353-362. doi: 10.1016/0021-9797(80)90304-5

47. Kakani V, Kim H, Basivi PK, Rasupuleti VR. Surface thermo-dynamic characterization of poly (vinylidene chloride-co-acrylonitrile) (P(VDC-co-AN)) using inverse-gas chromatography and investigation of visual traits using computer vision image processing algorithms. Polymers 2020; 12: 1631-1655. doi: 10.3390/polym12081631

48. Schultz J, Lavielle L, Martin C. The role of the interface in carbon fibre-epoxy composites. The Journal of Adhesion 1987; 23 (1): 45-60. doi: 10.1080/00218468708080469

49. Shi B, Wang Y, Jia L. Comparison of Dorris-Gray and Schultz methods for the calculation of surface dispersive free energy by inverse gas chromatography. Journal of Chromatography A 2011; 1218 (6): 860-862. doi: 10.1016/j.chroma.2010.12.050

50. Erol I, Cakar F, Ocak H, Cankurtaran H, Cankurtaran O, Bilgin-Eran B, Karaman F. Thermodynamic and surface characterization of 4-[4-((S)-citronellyloxy) benzoyloxy] benzoic acid thermotropic liquid crystal. Liquid Crystals 2016; 43 (1): 142-151. doi: 10.1080/02678292.2015.1067334

51. Gamelas JAF. The surface properties of cellulose and lignocellulosic materials assessed by inverse gas chromatography: a review. Cellulose 2013; 20: 2675-2693. doi: 10.1007/s10570-013-0066-5

52. Hamieh T, Abbasian A, Farshchi N. New methods to characterize the surface and interface acid-base properties of some hydrocarbons by inverse gas chromatography. Chromatographia 2020; 83: 615-629. doi: 10.1007/s10337-020-03878-z

53. Gutmann V. The Donor-Acceptor Approach to Molecular Interactions. New York, NY, USA: Plenum, 1978.

54. Yla-Maihaniemi PP, Heng JYY, Thielmann F, Williams DR. Inverse gas chromatographic method for measuring the dispersive surface energy distribution for particles. Langmuir 2008; 24(17): 9551-9557. doi: 10.1021/la801676n

55. Heydar KT, Pourrahim S, Ghonouei N, Yaghoubnejad S, Shatifi A. Thermodynamic parameters of a new synthesized tricationic ionic liquid stationary phase by inverse gas chromatography. Journal of Chemical & Engineering Data 2018; 63 (12): 4513-4523. doi: 10.1021/acs.jced.8b00601

56. Santos JMRCA, Guthrie JT. Study of a core-shell type impact modifier by inverse gas chromatography. Journal of Chromatography A 2005; 1070 (1-2): 147-154. doi: 10.1016/j.chroma.2005.02.060

57. Santos JMRCA, Guthrie JT. Analysis of interactions in multicomponent polymeric systems: the key-role of inverse gas chromatography. Materials Science and Engineering: R: Reports 2005; 50 (3): 79-107. doi: 10.1016/j.mser.2005.07.003

58. Gholami F, Tomas M, Gholami Z, Mirzaei S, Vakili M. Surface characterization of carbonaceous materials using inverse gas chromatography: a review. Electrochem 2020; 1: 367-387. doi: 10.3390/electrochem104002

59. Xu Y, Lin J, Xia J, Hu B. Surface characterization of urushiol-titanium chelate polymers by inverse gas chromatography. Chinese Journal of Chromatography 2011; 29 (3): 249-253. doi: 10.3724/sp.j.1123.2011.00249

60. Wang Q, Wang Q. Evaluation of the surface properties of poly (ionic liquid) materials by inverse gas chromatography. European Polymer Journal 2020; 123: 109451. doi: 10.1016/j.eurpolymj.2019.109451